Functional Model for Spacecraft Formation Flying using non-dedicated GPS/Galileo receivers

Peter J. Buist
Delft University of Technology
Delft, the Netherlands
Email: p.j.buist@tudelft.nl
Telephone: +31 (0)15 2782747
Fax: +31 (0)15 2783711

Peter J.G. Teunissen
Curtin University of Technology
Perth, Australia

Gabriele Giorgi
and Sandra Verhagen
Delft University of Technology
Delft, the Netherlands

***Abstract*—There is trend in spacecraft engineering toward distributed systems where a number of smaller spacecraft work as a larger multi-instrumented satellite. However, in order to make the small satellites work together as a single large platform, the precise relative positions and orientations of the elements of the formation have to be estimated. Global Navigation Satellite System (GNSS) receivers can be utilized to provide baseline estimates with centimeter to millimeter level accuracy. The legitimate spaceborne receivers can not be applied on smaller satellites due to various restrictions which are discussed in this paper, and therefore non-dedicated receivers are lately being used. However, to achieve precise relative positioning in situations with high dynamics and/or large receiver clock offsets, the standard functional model for GNSS-based relative positioning can not be applied. In the presented hardware-in-the-loop simulation of the Proba-3 spacecraft flying in formation, the error for the standard functional model can up to 16 centimeters. A new functional model is introduced that can correct the time-varying offset error and achieve the mm-level accuracy of GNSS even with non-dedicated GNSS receivers.**

I. Introduction

Formation flying a number of specialized small satellites instead of a single large multi-instrumented spacecraft can be advantageous for earth science applications. However, in order to make the satellites work as a single large platform it is normally required to know the relative positions and orientations of all the elements of the formation precisely. GNSS (GPS, Galileo, etc) can provide this information to the user down to centimeter or even millimeter level [1]. Currently, we are developing a method to rigorously integrate the attitude determination and relative positioning problems [2][3][4]. In this contribution we will extend the relative positioning part of the method for applications where the standard functional models for GNSS can not be applied. In section I-A and I-B, we will introduce the differences between legitimate spaceborne receivers and non-dedicated receivers applied onboard spacecraft. In section II, we will develop a functional model for precise relative positioning for formation flying with these non-dedicated receivers. In section III, the functional model is applied to the relative positioning problem and, in section IV, tested using hardware-in-the-loop experiments performed with the Formation Flying Testbed at the Navigational laboratory at ESTEC, the Netherlands. We will simulate a scenario with the orbital parameters of the Proba-3 mission with a short nominal inter-satellite distance (ISD) in a very eccentric orbit with an apogee of 71,200 km and a perigee of 800 km.

A. Spaceborne GNSS Receivers

A legitimate GNSS receiver developed for space applications is assembled from space qualified components and this inherently will make this kind of receiver more power hungry, heavier, bulky and costly compared to terrestrial receivers. On this type of receiver the larger frequency range of the Doppler shift is taken into account and most of the time the receiver clock is actively steered.
The topocentric distance is the distance between the user and the GNSS satellite in topocentric coordinates. The variation in topocentric distance between the distance at the GNSS system time and the receiver time is currently neglected in most applications; in other words the assumption is made that there is no motion of the receiver between system time and receiver time. For space applications, the influence of the affect is normally kept small by keeping the clock offset small, which is generally done in high-end space receivers as the Blackjack receiver [1] and the receiver developed for the Japanese space agency [5][6]. However if the clock error, as is usual in the non-dedicated GNSS receivers described in the next section, is not kept small and the standard model for relative positioning is applied, a time varying offset error is present in the solution as will be demonstrated in section IV.

B. Non-dedicated GNSS Receivers on Space Missions

On smaller satellites with mass, volume, power and cost constraints, the kind of receiver described in section I-A usually can not be applied and therefore a number of research groups have started to adjust terrestrial receivers for the space environment [7][8] or simply try to fly them in orbit [9].
As discussed, the variation in topocentric distance at the receiver and at the GNSS system time is currently neglected in most applications. Especially for most terrestrial applications, the variation due to motion of the receiver itself is very small. For a typical terrestrial user this affect is in the order of millimeters, especially if the receiver clock offset is

978-1-4244-8739-4/10/$26.00 ©2010 IEEE

actively steered. If this type of receiver is utilized for space applications, the variation in topocentric distance has to be taken into account. In the next section, we will develop a new functional model that does so.

II. Functional Model

A functional model describes the relationship between the observations and the unknown parameters. In this section, we will develop a new double difference model, where the variation in the tropocentric distance is taken into account. Subsection II-A, recaptures the RINEX instructions for correcting receiver clock offsets on the raw observations of the receiver. It will also explain why these instructions will not appropriately take the variation of the topocentric distance into account for GNSS receivers with high dynamics and/or large clock offsets. In subsection II-B, the new double difference model is derived. It is shown that the model can be simplified -under certain assumptions- to the standard double difference model.

A. RINEX instructions for correcting observations for clock errors

As was written in section I-A, we would ideally like to actively steer the receiver's clock. If this is not possible, we should use the absolute navigation result for correcting the GNSS observations according to the RINEX instructions [10][11]. The instructions are that if the receiver or the converter software adjusts the measurements using the real-time-derived receiver clock offsets *dT(r)*, the consistency of the three quantities phase / pseudo-range / epoch must be maintained, i.e. the receiver clock correction should be applied to all three observables:

Time(corr) = Time(r) - dT(r)

*PR(corr) = PR(r) - dT(r)*c*

*phase(corr) = phase(r) - dT(r)*freq*

where the *Time(r)* is the receiver time and *Time(corr)* is the time corrected for the offset from the GNSS time; *PR* is the pseudo range, *phase* is the carrier phase and *freq* is the observation frequency. *c* is the speed of light. However, for large clock offsets and/or high user dynamics, this correction might not capture the dynamics of the user(s) during the small time difference between receiver and system time, and thus only reduces the affects that will be described later in section IV. So the general discussion will remain valid even if the RINEX corrections are applied on the observations.

B. Deriving the Double Difference Model

In general, a code, phase and Doppler observation can be expressed by Eqs. (1), (2) and (3), respectively [12][13].

$$\begin{aligned} P^s_{r,f}(t) = {} & \rho^s_{r,f}(t, t-\tau^s_{r,f}) + I^s_{r,f} + T^s_{r,f} + \\ & + c\left[\zeta_r(t) - \zeta^s(t-\tau^s_{r,f})\right] + \\ & + c\left[d_{r,f}(t) + d^s_f(t-\tau^s_{r,f})\right] + \xi^s + e^s_{r,f} \end{aligned} \tag{1}$$

$$\begin{aligned} \Phi^s_{r,f}(t) = {} & \rho^s_r(t, t-\tau^s_{r,f}) - I^s_{r,f} + T^s_{r,f} + \\ & + c\left[\zeta_r(t) - \zeta^s(t-\tau^s_{r,f})\right] + \\ & + c\left[\delta_{r,f}(t) + \delta^s_f(t-\tau^s_{r,f})\right] + \lambda_f[\phi_{r,f}(t_0) + \phi^s_f(t_0)] + \\ & + \lambda_f N^s_{r,f} + \xi^s + \varepsilon^s_{r,f} \end{aligned} \tag{2}$$

$$\begin{aligned} D^s_r(t) = {} & \dot{\rho}^s_r(t, t-\tau^s_{r,f}) - \dot{I}^s_{r,f} + \dot{T}^s_{r,f} + \\ & + c\left[\dot{\zeta}_r(t) - \dot{\zeta}^s(t-\tau^s_{r,f})\right] + \dot{\xi}^s + \dot{\varepsilon}^s_{r,f} \end{aligned} \tag{3}$$

where $(..)^s_{r,f}$ means between receiver r and satellite s on frequency f

$P^s_{r,f}$	Code observation
t	Observation time
ρ^s_r	the geometric distance between r at time t and s at time $t-\tau^s_{r,f}$
$\tau^s_{r,f}$	The signal traveling time
$T^s_{r,f}$	Tropospheric error at f
$I^s_{r,f}$	Ionospheric error at f
ζ_r	Clock error of r
ζ^s	Clock error of s
d^s_f	Instrumental code delay for s on f
$d_{r,f}$	Instrumental code delay for r on f
ξ^s	Satellite's ephemeris error
e	Residual unmodelled error terms for the code observations
$\Phi^s_{r,f}$	Carrier phase observation
$\phi_{r,f}(t_0)$	Initial phase at frequency f in r
$\phi^s_f(t_0)$	Initial phase of carrier phase $L = \frac{f}{c}$ in s
δ^s_f	Instrumental phase delay for s on L
$\delta_{r,j}$	Instrumental phase delay for r on L
$N^s_{r,f}$	Number of complete carrier phase cycles that have occurred prior to the signal's arrival at the antenna
ε	Residual unmodelled error terms on the carrier phase observations
$D^s_{r,f}$	Doppler observations

The notation $\dot{(..)}$ indicates the time derivatives of quantity $(..)$, as there are geometric distance ρ^s_r, ionospheric $I^s_{r,f}$ and tropospheric $T^s_{r,f}$ errors, the receiver ζ_r and satellite clock ζ^s error, ephemeris error ξ^s and residual error ε. The Doppler observation is normally generated from carrier phase observations, therefore the last term of Eq. (3), the unmodelled error term $\dot{\varepsilon}^s_{r,f}$, is the derivative of the error $\varepsilon^s_{r,f}$ in Eq. (2).

The Eq. (1) and (2) can be linearized as described in [12]. For

Eq. (3) using

$$\frac{\partial}{\partial t}\left(\frac{\partial \rho^s_{r,f}(t,t-\tau^s_{r,f})}{\partial \mathbf{r}_r}\Big|_0 \triangle \mathbf{r}_r\right) = \frac{-\partial(\mathbf{u}^s_r \triangle \mathbf{r}_r)}{\partial t} = -\dot{\mathbf{u}}^s_r \triangle \mathbf{r}_r - \mathbf{u}^s_r \triangle \dot{\mathbf{r}}_r \quad (4)$$

where $\mathbf{r}_r$ is the user position, $\mathbf{u}^s_r$ is the transpose of the line-of-sight vector from the receiver r to satellite s, $\triangle \mathbf{r}_r$ is the increment of the position vector and $\triangle \dot{\mathbf{r}}_r$ its derivative, we obtain a linear equation relating the receiver position, velocity vectors and the clock drift to the Doppler observations.
By taking the differences between two receivers and the GNSS satellites, the double difference model can be derived. In this model, we make use of the following notation to write the single difference range rate:

$$\dot{\rho}^{s_{12}}_{r1} = \left[\dot{\rho}^{s_1}_{r1}(t,t-\tau^{s_1}_{r1,f}) - \dot{\rho}^{s_2}_{r1}(t,t-\tau^{s_2}_{r1,f})\right]$$
$$\dot{\rho}^{s_{12}}_{r2} = \left[\dot{\rho}^{s_1}_{r2}(t,t-\tau^{s_1}_{r2,f}) - \dot{\rho}^{s_2}_{r2}(t,t-\tau^{s_2}_{r2,f})\right]$$

And thus the proposed double difference model becomes:

$$\triangle P^{s_{12}}_{r_{12},f} = -\mathbf{u^{s_{12}}_{r_2}} \triangle \mathbf{r}_{r_{12}} - \dot{\rho}^{s_{12}}_{r1} \triangle \zeta_{r_1} + \dot{\rho}^{s_{12}}_{r2} \triangle \zeta_{r_2} + + I^{s_{12}}_{r_{12},f} + T^{s_{12}}_{r_{12},f} + e^{s_{12}}_{r_{12},f} \quad (5)$$

$$\triangle \Phi^{s_{12}}_{r_{12},f} = -\mathbf{u^{s_{12}}_{r_2}} \triangle \mathbf{r}_{r_{12}} - \dot{\rho}^{s_{12}}_{r1} \triangle \zeta_{r_1} + \dot{\rho}^{s_{12}}_{r2} \triangle \zeta_{r_2} + - I^{s_{12}}_{r_{12},f} + T^{s_{12}}_{r_{12},f} + \lambda_f N^{s_{12}}_{r_{12},f} + \varepsilon^{s_{12}}_{r_{12},f} \quad (6)$$

$$\triangle D^{s_{12}}_{r_{12},f} = -\mathbf{u^{s_{12}}_{r_2}} \triangle \dot{\mathbf{r}}_{r_{12}} - \dot{\mathbf{u}}^{s_{12}}_{r_2} \triangle \mathbf{r}_{r_{12}} + - \dot{I}^{s_{12}}_{r_{12},f} + \dot{T}^{s_{12}}_{r_{12},f} + \dot{\varepsilon}^{s_{12}}_{r_{12},f} \quad (7)$$

These equations show that, different from the standard double difference model, in the new model the receiver clock errors do not completely disappear from the Eq. (5) and (6). By neglecting these receiver clock error terms, the standard double difference model, without the Doppler observations, used in terrestrial surveying [12], but also for relative positioning in the space environment [1], is obtained:

$$\triangle P^{s_{12}}_{r_{12},f} = -\mathbf{u^{s_{12}}_{r_2}} \triangle \mathbf{r}_{r_{12}} + I^{s_{12}}_{r_{12},f} + T^{s_{12}}_{r_{12},f} + e^{s_{12}}_{r_{12},f} \quad (8)$$

$$\triangle \Phi^{s_{12}}_{r_{12},f} = -\mathbf{u^{s_{12}}_{r_2}} \triangle \mathbf{r}_{r_{12}} + - I^{s_{12}}_{r_{12},f} + T^{s_{12}}_{r_{12},f} + \lambda_f N^{s_{12}}_{r_{12},f} + \varepsilon^{s_{12}}_{r_{12},f} \quad (9)$$

In the next section, we will test both models with data collected from two platform moving with high dynamics in a very eccentric orbit.

III. Relative Positioning

Standard relative positioning models use two types of observations: pseudo range and carrier phase. In this section we will introduce a model that makes use of these two observations plus Doppler. The double difference observation equations were derived in section II-B. The pseudo range observations can have an accuracy of meters to decimeters [14] and the carrier phase observations have accuracies down to millimeter level. The Doppler observation have an accuracy worse than carrier phase but normally better than centimeter level [13].

A. Standard Model

The double difference observation equations, Eq. (8) and (9) can be written for a single baseline as a system of linearized observation equations [12]:

$$E(y) = Az + Gb, \quad D(y) = Q_{yy} \quad (10)$$

where E is the expected value and D is the dispersion of y. y is the vector of observed minus computed double difference carrier phases and code observations of the order $m = 2n$, z is the unknown vector of ambiguities of the order n expressed in cycles rather than range to maintain their integer character. b is the baseline vector of order three. G is the geometry matrix containing normalized line-of-sight vectors, A is a design matrix that links the data vector to the unknown vector z. The variance matrix of y is given by the positive definite matrix Q_{yy} which is assumed to be known. In our notation we will make use of the weighted squared norm $\|..\|^2_{Q_{yy}} = (..)^T Q^{-1}_{yy}(..)$.
It is important to note that the ambiguities are integers and therefore z and b are ($z \in \mathbb{Z}^n, b \in \mathbb{R}^3$) with $\mathbb{Z}^n$ being the $n-$dimensional space of integers. The set of linear observation equations is solved by applying the well-known LAMBDA method [15] on the Integer Least-Squares problem with the least-squares criterion:

$$\min_{z\in\mathbb{Z}^n, b\in\mathbb{R}^3} \|y - Az - Gb\|^2_{Q_{yy}} \quad (11)$$

B. Proposed Model

For our proposed model, we will make use of the vector υ of n observed minus computed double difference carrier phases, code and Doppler observations, as described by Eq. (5), (6) and (7), of the order $m = 3n$. β contains the baseline vector b of order three, and its derivative $\dot{b}$ with the same order, which is the relative velocity between the two platforms, thus $\beta = [b, \dot{b}]^T$. Γ contains the geometry matrix of normalized line-of-sight vectors G and its derivative $\dot{G}$: $\Gamma = \begin{bmatrix} G & 0 \\ \dot{G} & G \end{bmatrix}$. A is the design matrix that links the data vector to the unknown vector z. Applying this notation and $\triangle\zeta_r$ as a-priori information from the absolute positioning result for each receiver, the double difference observation equations, Eqs. (5), (6) and (7), can be written for a single baseline as a system of linearized observation equations:

$$E(\upsilon) = Az + \Gamma\beta, \quad D(\upsilon) = Q_{\upsilon\upsilon} \quad (12)$$

The ambiguities are integers and therefore z and β are ($z \in \mathbb{Z}^n, \beta \in \mathbb{R}^{1\times 6}$). The least-squares criterion for the problem reads as:

$$\min_{z\in\mathbb{Z}^n, \beta\in\mathbb{R}^{1\times 6}} \|\upsilon - Az - \Gamma\beta\|^2_{Q_{\upsilon\upsilon}} \quad (13)$$

TABLE I
ORBIT SPECIFICATION FOR THE FORMATION FLYING SPACECRAFT

Orbital Period	± 24.1 hours
Apogee (altitude)	77,578 (71,200) km
Perigee (altitude)	7,178 (800) km
Inclination	17.8°
Mean Anomaly at start of simulation	352°
Nominal ISD	0.150 km

Now again we can obtain, using the same approach as described in section III-A, the Integer Least Solution by applying the LAMBDA method, as described in [15].

IV. SATELLITE FORMATION FLYING: PROBA-3

In this section, we will test the standard and proposed model using data collected in an experiment of two satellites flying in close formation.

A. Hardware-in-the-loop Simulation Setup

In this contribution we will use the same hardware-in-the-loop experimental setup performed with the Formation Flying Testbed at the Navigational laboratory at ESTEC, the Netherlands, as described in [3] and [4]. In this formation flying experiment, two spacecraft are simulated with on each spacecraft a PolaRx2@ receiver [16]. Both satellites have, in addition to the master antenna, two single frequency auxiliary antennas. In this paper, observations from these single frequency antennas are not applied, but in [2][3][4] it was shown how this data can be utilized to enhance the relative positioning. A scenario was simulated with the orbital parameters of the Proba-3 mission as shown in Table I and a nominal inter-satellite distance (ISD) of 150 meter. For the Proba-3 scenario only the part of orbit where the satellites are below the GPS constellation was simulated (see Fig. 1), as the PolaRx2@ receivers are not modified for an orbit higher than the GPS constellation. According to [17], this matches well with the real mission requirements as the relative GPS equipment will be used during the period where the satellites are below 5000 km. The velocity of the satellites passing through the perigee is about 10 km/s (≈40.000 km/hr).

In Fig. 2 the simulation set-up at the ESTEC navigation laboratory is shown, consisting of one Spirent GPS simulator (4760) with three rf outputs and two Septentrio Polarx2@ receivers, adjusted to acquire and track the GPS signals in a LEO environment. More information about the test set-up can be found in [17].

B. Experimental Results

1) Relative Positioning using standard Double Difference Model with pseudo range and carrier phase observations: Fig. 3 and Fig. 4 contain results, obtained from a hardware-in-the-loop experiment for the PROBA-3 mission, which was described in detail in section IV. Fig. 3 shows the the clock offsets for the receivers obtained from the absolute position estimate for receiver 1 (Clk1) and receiver 2 (Clk2). In Fig. 3

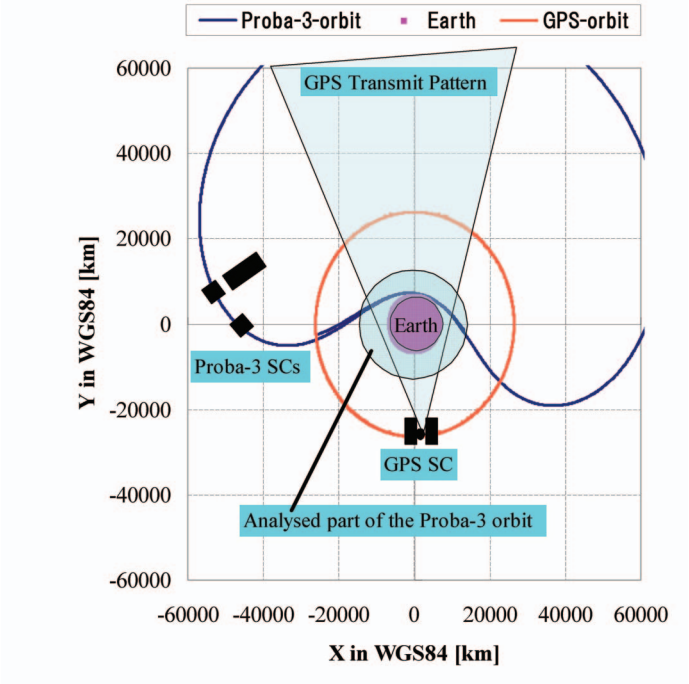

Fig. 1. Orbits of Proba-3 and GPS spacecraft (SC)

we see that clocks of the two receivers in this experiment behave very differently. The clock drift of Clk2 is much larger than the drift of Clk1. The clocks of the two receivers are controlled within 0.5 ms; if one of the two clock errors exceeds this threshold it is steered. Fig. 4 shows the error in the baseline estimation if the standard double difference model, as described by Eq. (10), is applied. By comparing Fig. 3 and Fig. 4, we observe that the baseline error is related to the relative clock error as described by Clk1-Clk2. But the relationship is not linear; there is a second affect in the baseline error that is related to the relative dynamics between the GNSS satellite and the user(s). This will be investigated in the next section.

At the instant the clock is steered, also the baseline error is changing. The maximum baseline error is around 16 centimeter with the standard double difference model and the error

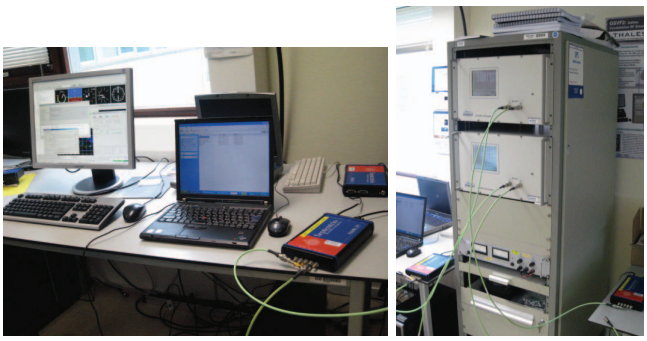

Fig. 2. GPS Simulator and Receivers

depends on the difference between clock offsets of the two receivers and the user dynamics. This results in a time-varying offset in the relative position or baseline estimate between the two receivers. Table II shows that the mean error μ and standard deviation σ on the baseline estimate are 14.90 mm and 42.07 mm respectively.

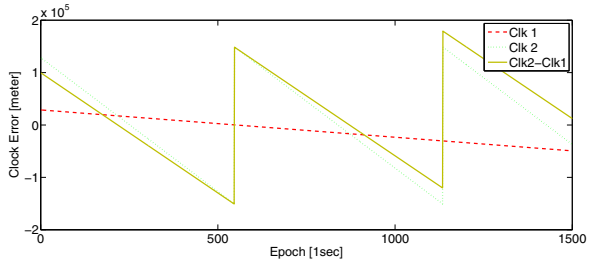

Fig. 3. Clock errors and the difference for the two GPS receivers

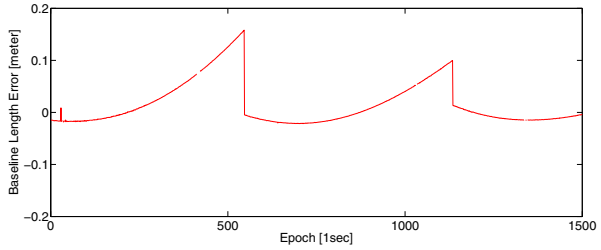

Fig. 4. Baseline error using the standard double difference model

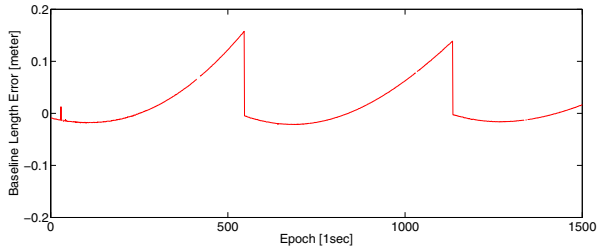

Fig. 5. Baseline error using the proposed double difference model only for receiver 1

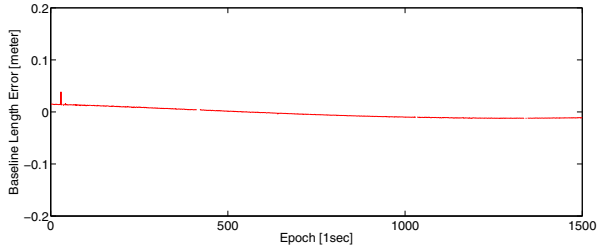

Fig. 6. Baseline error using the proposed double difference model only for receiver 2

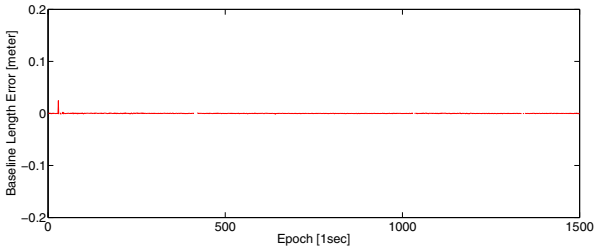

Fig. 7. Baseline error using the proposed double difference model for both receivers

TABLE II
MEAN μ AND STANDARD DEVIATION σ FOR THE BASELINE ESTIMATE

	Relative Positioning Error [mm]	
	μ	σ
Standard Model	14.90	42.07
Proposed Model	0.05	0.70

2) Relative Positioning using the proposed Double Difference Model with pseudo range, carrier phase and Doppler Observations: In Fig. 5, Fig. 6 and Fig. 7, we apply the proposed double difference Model as described by Eq. (12). In Fig. 5 only corrections, based on clock error and range rate, are made for receiver 1, in Fig. 6 only for receiver 2 and in Fig. 7 for both receivers. As receiver 1 has only a small clock offset, in Fig. 5 not much difference is observed compared to Fig. 4. Receiver 2 has a much larger time offset, therefore the baseline estimate in Fig. 6 is much improved and a small error - almost linearly depending on the clock offset of receiver 1 - becomes apparent. In Fig. 7, corrections are applied for both receivers and the time-varying offset error in the baseline estimate is completely removed. By comparing Fig. 7 with Fig. 4, we conclude that the proposed double difference model can correct the clock behavior and dynamics of the receivers well. The results, if corrections from both receivers are applied, are summarized in Table II. The mean error and standard deviation on the baseline estimate are 0.05 mm and 0.7 mm respectively. So the mean of the error is almost zero and the standard deviation is approaching the theoretical limit of GNSS relative positioning.

V. CONCLUSION

In this contribution, we have developed a new functional model, in which the variation between the topocentric distance at the GNSS system time and at the GNSS receiver time is taken into account. For users with high dynamics and/or large clock offsets, not taking this affect into account can cause time-varying offsets in the baseline estimate. In the hardware-in-the-loop simulation presented in this paper of the Proba-3 spacecraft flying in formation in a very eccentric orbit, this error can be up to 16 centimeters. In the proposed functional model, this error can be corrected and the accuracy of the baseline estimate approaches the theoretical limitation.

ACKNOWLEDGMENT

The GPS simulators and receivers used for the test have been provided by the navigation laboratory of the European Space Agency (ESA-ESTEC). The authors would like to thank the people from this laboratory, especially Alberto Garcia-Rodríguez, Jaron Samson and David Jeménez Banos, for their support. Professor Teunissen is the recipient of an Australian Research Council Federation Fellowship (project number FF0883188). This work has also been done in the context of the Australian Space Research Program project: SAR Formation Flying. The research of Sandra Verhagen is supported by the Dutch Technology Foundation STW, applied science division of NWO and the Technology Program of the Ministry of Economic Affairs. All this support is greatly acknowledged.

REFERENCES

[1] R. Kroes, O. Montenbruck, W. Bertiger, and P. Visser, "Precise GRACE baseline determination using GPS," *GPS Solutions*, vol. 9, no. 1, pp. 21–31, 2005.

[2] P. J. Buist, P. J. G. Teunissen, G. Giorgi, and S. Verhagen, "Multiplatform Instantaneous GNSS Ambiguity Resolution for Triple- and Quadruple-Antenna Configurations with Constraints," *International Journal of Navigation and Observation, vol. 2009, Article ID 565426, 14 pages, doi:10.1155/2009/565426*, 2009.

[3] P. J. Buist, P. J. G. Teunissen, S. Verhagen, and G. Giorgi, "Attitude Bootstrapped Relative Positioning for Spacecraft," *Proceedings of Fourth European Workshop on GNSS Signals and Signal Processing GNSS SIGNALS 2009, 10-11 December 2009, Oberpfaffenhofen, Germany*, 2009.

[4] ——, "A Vectorial Bootstrapping Approach for Integrated GNSS-based Relative Positioning and Attitude Determination of Spacecraft," *Acta Astronautica, doi:10.1016/j.actaastro.2010.09.027*, 2010.

[5] S. Kumagai, T. Ito, K. Toda, and T. Iwata, "Precision GPS Receiver for the Advanced Land Observing Satellite (ALOS)," *Proceedings of the Space Sciences and Technology Conference, in Japanese*, vol. 45, pp. 131–135, 2001.

[6] P. J. Buist, S. Kumagai, M. Kasahara, K. Ijichi, K. Hama, and S. Nakamura, "Flight Experience of Single and Dual Frequency GPS Receivers Onboard of SERVIS-1 and USERS Satellites," *Proceedings of NAVITEC, Noordwijk, the Netherlands*, 2004.

[7] M. Unwin, M. Oldfield, C. Underwood, and R. Harboe-Sorensen, "The use of commercial technology for spaceborne GPS receiver design," pp. 1983–1989, 1998.

[8] R. Langley, O. Montenbruck, M. Markgraf, C. Kang, and D. Kim, "Qualification of a commercial dual-frequency GPS receiver for the e-POP platform onboard the Canadian CASSIOPE spacecraft," pp. 8–10, 2004.

[9] H. Saito, T. Mizuno, K. Kawahara, Y. Tsuda, K. Shinkai, T. Saiki, Y. Fukushima, Y. Hamada, H. Sasaki, S. Katsumoto *et al.*, "Development and On-Orbit Results of Miniature Space GPS Receiver by means of Automobile-Navigation Technology," *IEIC Technical Report (Institute of Electronics, Information and Communication Engineers)*, vol. 106, no. 217, pp. 17–22, 2006.

[10] W. Gurtner and L. Estey, "RINEX: The Receiver Independent Exchange Format, Version 2.11," 2006.

[11] ——, "RINEX: The Receiver Independent Exchange Format, Version 3.00," 2006.

[12] P. J. G. Teunissen and A. Kleusberg, "GPS for Geodesy," *Springer, Berlin Heidelberg New York*, 1998.

[13] P. Misra and P. Enge, *Global Positioning System: Signals, Measurements, and Performance*. Ganga-Jamuna Press, Lincoln MA, 2001.

[14] P. J. Buist, P. J. G. Teunissen, G. Giorgi, and S. Verhagen, "Multivariate Bootstrapped Relative Positioning of Spacecraft Using GPS L1/Galileo E1 Signals," *Advances in Space Research, special issue: Galileo, doi:10.1016/j.asr.2010.10.001*, 2010.

[15] P. J. G. Teunissen, "The Least-Squares Ambiguity Decorrelation Adjustment: a Method for Fast GPS Integer Ambiguity Estimation," *Journal of Geodesy*, vol. 70, pp. 65–82, 1995.

[16] J. Leyssens and M. Markgraf, "Evaluation of a Commercial-Off-The-Shelf dualfrequency GPS receiver for use on LEO satellites," *Proceedings of the 18th International Technical meeting of the Institute of Navigation Satellite Division, ION-GNSS-2005, Long Beach, CA, US, September 13-16*, 2005.

[17] M. Manzano-Jurado, C. Carrascosa-Sanz, and A. Garcia-Rodrígues, "Formation Flying LEO Test Bed at the ESTEC Navigation Laboratory," *4rd ESA Workshop on Satellite Navigation User Equipment Technologies, NAVITEC, Noordwijk, The Netherlands, December 10-12*, 2008.